Alloy Films Deposited by Electroplating as Precursors for Protective Oxide Coatings on Solid Oxide Fuel Cells Metallic Interconnect Materials

Christopher Johnson, Randall Gemmen, Caleb Cross

DOE/NETL, 3610 Collins Ferry Rd, Morgantown, WV, 26507

Interconnect, Coating, Spinel, SOFC, electroplating

Abstract

The successful development of stainless steel interconnects for intermediate temperature solid oxide fuel cells (SOFC) may be the materials breakthrough that makes SOFC technology truly commercial. Many of the ferritic stainless steels, however, suffer from a relatively high area specific resistance (ASR) after long exposure times at temperature and the Cr in the native oxide can evaporate and contaminate other cell components. Conductive coatings that resist oxide scale growth and chromium evaporation may prevent both of these problems. In the present study electrochemical deposition of binary alloys followed by oxidation of the alloy to form protective and conductive oxide layers is examined. Results are presented for the deposition of Mn/Co and Fe/Ni alloys via electroplating to form a precursor for spinel oxide coating formation. Analysis of the alloy coatings is done by SEM, EDS and XRD.

Introduction

Solid oxide fuel cells (SOFC) hold great potential for future electrical energy production (1). This is not only because SOFC are more efficient than current commercial methods of electricity production, but also because they emit lower levels of pollutants than these alternative methods. The high operating temperature of SOFC relative to other types of fuel cells also make them ideal for combined cycle SOFC/ turbine applications, where efficiency may approach 70-80%. At typical operating temperatures (700-1000ºC), internal reforming of hydrocarbon fuels using their excess heat is also a possibility. The impediments to commercialization are related to a number of cell and stack materials issues. Reliable and effective seals, Ni/YSZ anode materials that can survive hydrocarbon gas mixtures, and low cost interconnects for planar SOFC, are examples of issues still being investigated. This work focuses on the development of low cost and effective interconnects for planar SOFC.

The recent lowering of the typical operating temperature needed for SOFC operation means that a number of lower cost materials have become potential replacements for previously used materials. One such opportunity is the replacement of the $LaCrO_3$ based ceramic interconnects with low cost high temperature alloys(2). Besides lower cost, the high temperature alloys also have the added benefit of higher mechanical strength and higher thermal conductivity. The best candidate high temperature alloys are chromia formers. This is because chromia has the lowest electronic resistivity relative to other native oxides of high temperature alloys. However, chromia scales are not as resistant to oxide growth at elevated temperatures as the alumina formers, and thus over the long term the oxide scales continue to grow and

increase resistance. In addition, in the severe SOFC cathode environment, volatile Cr species can migrate and contaminate the cathode/electrolyte interface, causing degradation of cell performance. Thus, while the high temperature chromia forming alloys are the best replacement candidates for $LaCrO_3$ based SOFC interconnects, additional improvement in corrosion resistance and a solution to the chromia volatility issue remain to be addressed.

Potential mitigations for the problems with the chromia forming alloys includes, adjustment of the alloy composition such that a better native oxide forms(3,4), surface modification of the alloy composition for the same reason, and coatings that provide better oxidation resistance and decrease chromia volatility(5,6,7). In this work we report our initial efforts to obtain coatings via electroplating methods. Electroplating of alloys or individual metals followed by controlled oxidation and/or reaction to the desired phase may be a cost effective method for the formation of dense coatings. This method may also be more effective as a method of coating on interconnects with complex geometries or even deposition on internal pores of foam materials. This report primarily looks at the deposition of a Mn/Co and NiFe alloys from single deposition solutions on stainless steel substrates and some initial work on the oxidation process. Characterization of the deposits and oxidized samples is by SEM ,EDS and XRD.

Experimental

The electrolytes used in this experiment were prepared from $CoSO_4 \bullet 7H_20$, $MnSO_4 \bullet H_2O$, $NiSO4 \bullet 6H_2O$, $FeSO_4 \bullet 7H_2O$, saccharin, and disodium EDTA. Dilute sulfuric acid (H_2SO4) and sodium hydroxide (NaOH) were used to adjust pH. All solutions were made with deionized water. The deposition cell used the work piece (crofer APU 22 alloy, or Haynes 230) as the cathode, and two sheets of platinum mesh were used as the anodes. The fixture was suspended in a beaker of the solution and this was placed on a heating and stirring mantle, and a Teflon coated stir bar used to provide agitation. These experiments were done without the use of a reference electrode. All experiments were carried out at 50 °C. The morphology and composition of the deposited samples were analyzed using a JEOL JSM 6300 FE-SEM equipped with a Thermo Electron EDS system. Oxidation was at 800 °C in air. XRD analysis was done using a Panalytical Xpert Pro system in 2theta geometry.

Results and Discussion

The effect of the saccharin additive was investigated by depositing single metal Co and Mn electrodeposited from simple single component ($CoSO_4 \bullet 7H_20$ or $MnSO_4 \bullet H_2O$) solutions with and without saccharin additive. For the cobalt deposition the concentration of cobalt sulphate was 0.1M and saccharin was 0.0025M. The cell was operated potentiostatically at an applied voltage of 4V. Figure 1 shows the SEM images of the results found for the Co deposition. The left image shows the morphology of the cobalt deposit when saccharin additive is not present. The bright large nodules grown on the surface are pure cobalt, and the dark surrounding regions are the substrate with no deposition of cobalt. The image on the right shows the effect of addition saccharin to the deposition solution. This SEM image (along with EDS analysis) confirms that the cobalt has deposited relatively uniformly over the surface of the substrate with only an occasional cobalt cluster present (the light particles intermittently dotting the surface). Because of the continued formation of a few cobalt clusters the saccharin concentration was raised to 0.0075M for the remainder of the experiments. The effect of saccharin addition on the deposition of Mn is qualitatively similar. The morphology of the Mn is significantly smoother when saccharin is added.

The deposition of alloys by simple DC methods can only be accomplished when the deposition potential for each of the components are approximately the same. The standard reduction potentials for
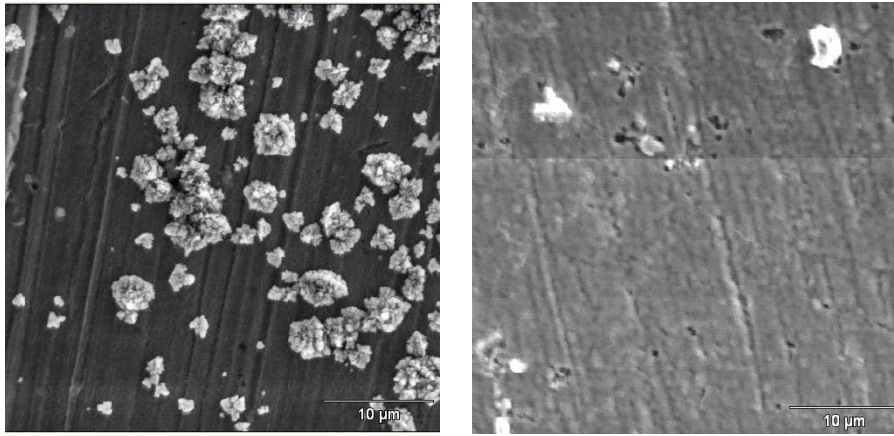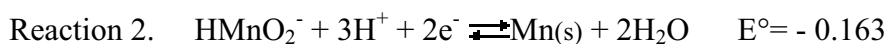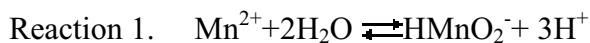
Figure 1. SEM images of deposits of Co on metallic substrates. The image on the left is of a deposit of Co from a simple solution of $CoSO_4$, and the image on the right shows the same deposition product, except that 0.0025M saccharin has been added to the solution.

Mn^{2+} and Co^{2+} are -1.180V and - 0.277V respectively, and the standard reduction potentials for Ni^{2+} and Fe^{2+} are -0.250V and -0.440V respectively. The larger difference in standard reduction potential for the Mn/Co suggests that this alloy may be more difficult to deposit in a controlled fashion. For instance, estimation of the concentrations necessary to bring the deposition potentials to equal levels for Mn^{2+} and Co^{2+} done using the Nernst equation and assuming dilute solutions (so that concentration can be used instead of activity) shows that the Co^{2+} concentration would need to be approximately 30 orders of magnitude more dilute than the Mn^{2+} ion concentration. In the case of the Ni/Fe alloy deposited using Ni^{2+} and Fe^{2+} the concentration difference only needs to be 6 orders of magnitude concentration difference to obtain a 50/50 alloy mixture to occur. However, while we then expect the Ni/Fe alloy deposition to require less manipulation in order to obtain the desired alloy composition, both systems cannot be controlled strictly by controlling concentration of the deposition solution, and therefore alternative methods of controlling the deposition potentials need to be found.

One method of changing the deposition potential for a given metal is to change the species from which the deposition is made. This can be done by formation of a complex or species with a higher or lower standard reduction potential. For instance, EDTA has been used in Zn-Mn alloy electroplating to change the deposition potential of the Zn^{2+} species(8). The Zn^{2+} was reacted with stoichiometric amounts of EDTA to form an EDTA-Zn complex before the remaining Mn species was added to the solution. The result is an increase in the deposition potential of the Zn species at a given concentration. For the purposes of this study EDTA may be used to complex the cations with lower deposition potentials (Ni^{2+}, Co^{2+}) and thus raise their effective deposition potentials relative to the higher standard reduction potential cations(Fe^{2+},Mn^{2+}). It is expected that the chelation of the Ni^{2+} ion with EDTA will be sufficient to allow only minor concentration variation of the Fe^{2+} concentration such that successful Ni/Fe alloy coatings may be obtained. However, in the case of Mn/Co alloy deposition this step alone may not be sufficient to create compositional control of the alloy.

Reaction 1. $Mn^{2+} + 2H_2O \rightleftharpoons HMnO_2^- + 3H^+$

Reaction 2. $HMnO_2^- + 3H^+ + 2e^- \rightleftharpoons Mn_{(s)} + 2H_2O$ $E° = - 0.163$

To lower the deposition potential of the Mn^{2+} species in the Mn/Co deposition solution we can take advantage of the effect of pH on the presence of a more easily reducible aqueous manganese species

(shown in reaction 1) created when Mn^{2+} ions are dissolved in water. The standard reduction potential of $HMnO_2^-$ (shown along with the deposition reaction, reaction 2) is -0.163V, much lower than -1.180V for the Mn^{2+} species. The K_{sp} of the reaction shown below at 50°C is $6.59X10^{-19}$, thus under typical conditions (when the $MnSO_4$ is simply added to solution) the $HMnO_2^-$ concentration is very low and despite the lower E° value for this species the deposition potential remains high because of the low concentration. However, we can shift the concentration of the deposition species by changing the pH, that is, by consuming the H^+ ions available in solution we can shift the equilibrium for reaction 1 to the right and increase the amount of $HMnO_2^-$ available for deposition. The concentration of $HMnO_2^-$ species can be calculated at a number of pH values by use of the equilibrium equation below.

$$K = \frac{[HMnO_2^-][H^+]^3}{[Mn^{2+}]} = 1.6X10^{-32}$$

Then by substituting these concentration values into the Nernst equation the deposition potential for $HMnO_2^-$ at a number of pH values can be estimated for a given manganese sulfate concentration. Figure 2 shows the calculated deposition potential for $HMnO_2^-$ to Mn(s) as in reaction 2 over a range of pH values. Again, it is assumed that concentrations can be substituted for activities in the Nernst equation. Note that at very high pHs the value of the deposition potential approaches the deposition potential of Co^{2+} (- 0.277V), which would suggest that simply increasing the pH near 9 would lead to alloy deposition without complexation of the Co^{2+} with EDTA. Unfortunately, at pH levels approaching 8, precipitation of hydroxide occurs in the solution, therefore it is still necessary to increase the deposition potential of the Cobalt ion.
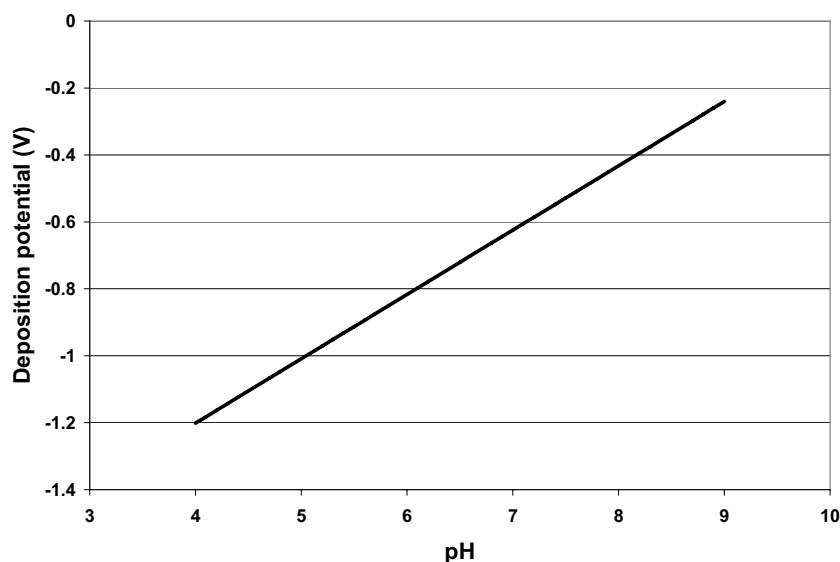

Figure 2. The Calculated deposition potential as a function of pH for deposition of Mn(s) from $HMnO_2^-$ containing solutions, using the Nernst equation and assuming dilute solutions.

Given the above information we determined that we would first dissolve the low standard reduction potential cations into solution, and then add stoichiometric amounts of EDTA to chelate the Ni^{2+} and Co^{2+} prior to adding the Fe^{2+} and Mn^{2+} for the respective deposition solutions. The saccharin was also added after the chelation of the Co^{2+} and Ni^{2+} cations. In the Mn/Co deposition solution the pH was controlled using 10% solutions of H_2SO_4 and NaOH. Figure 3 shows the Mn/Co atomic ratio of the deposited films as a function of pH. In this case the cell was operated galvanostatically at 50mA. It should also be pointed out that at the pH of 8 a small amount of precipitate was present in the solution.

Nevertheless, from this graph, we can see that to obtain a 50/50 mixture of Co and Mn in the deposited alloy from this particular solution, the pH should be near 7.5. However, care must be taken when operating the cell above a voltage that can dissociate water as the half reaction at the cathode for water electrolysis also creates hydroxide ions. Thus localized increases in pH can occur and produce significant amounts of hydroxide precipitate on the work piece. Only a single deposition solution has been attempted thus far for the Ni/Fe alloy deposition. The concentrations in the deposition solution were 0.1 molar NiSO4, EDTA and FeSO4, and 0.0075 molar saccharin. At 5 volts DC applied cell voltage, this resulted in an alloy film with approximately 25% Ni and 75% Fe.
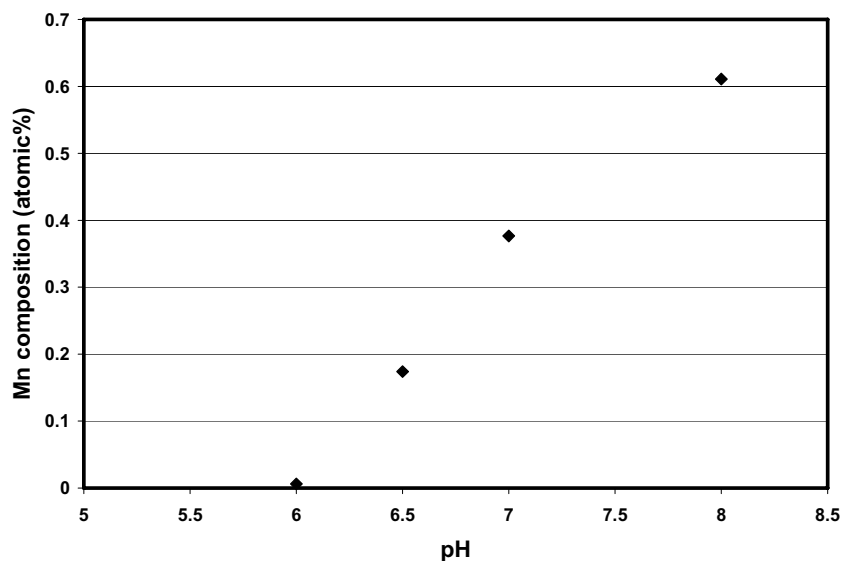

Figure 3. Mn composition as a function of pH using a solution containing 0.008M CoSO4, 0.008M EDTA, 0.075M Saccharin, 0.032M $MnSO_4$. In this case the cell was operated galvanostatically at 50mA.

Oxidation of the samples was done in air at 800C for two hours. Figure 4 and figure 5 show the XRD data collected after oxidation on a Mn/Co alloy and a Ni/Fe alloy coated samples respectively. Note that in both figures spinel phase has been detected by the XRD. At this time it is not clear whether we have obtained the desired spinel phases from the alloy coatings. In order to clarify what the composition of the oxide layers further analysis by cross section SEM/EDS will done in the future. However from the specific lattice parameters calculated for the spinels we can say that in the case of the Mn/Co alloy coating the spinel formed upon oxidation is more consistent with Fe_3O_4 spinel. For the Ni/Fe alloy coating after oxidation the lattice parameters are consistent with the formation of the $NiFe_2O_4$ spinel. Clearly however, since many of the elements present at the surface can form solid solutions of spinels, we can not be certain until we have measured the oxide coating composition by another means. Note also that Cr_2O_3 is detected

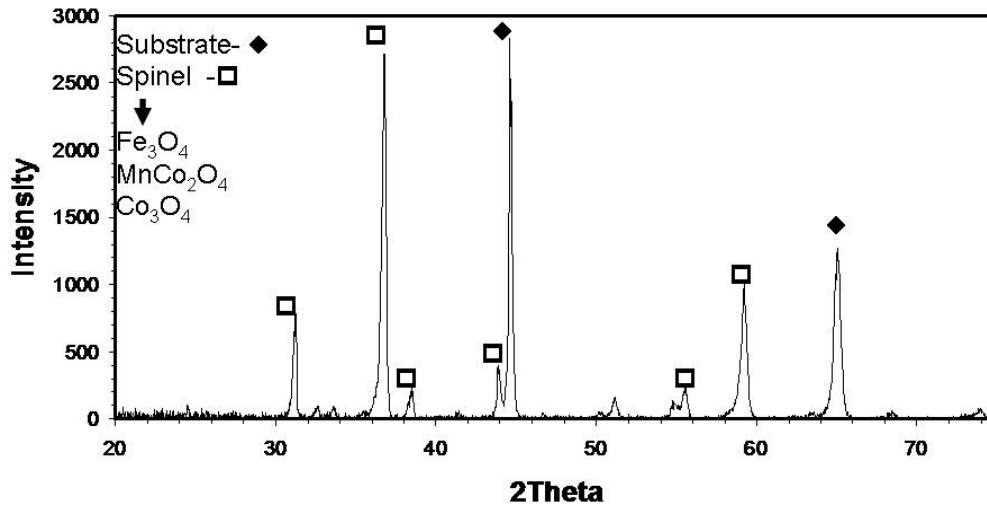as a second phase for the Ni/Fe alloy sample, and that a number of unidentified minor peaks are present.

Figure 4. X-Ray Diffraction pattern of an Mn/Co alloy coated Crofer 22 APU sample with the alloy having a composition of 45% Mn and 55% Co after heating in air to 800°C.
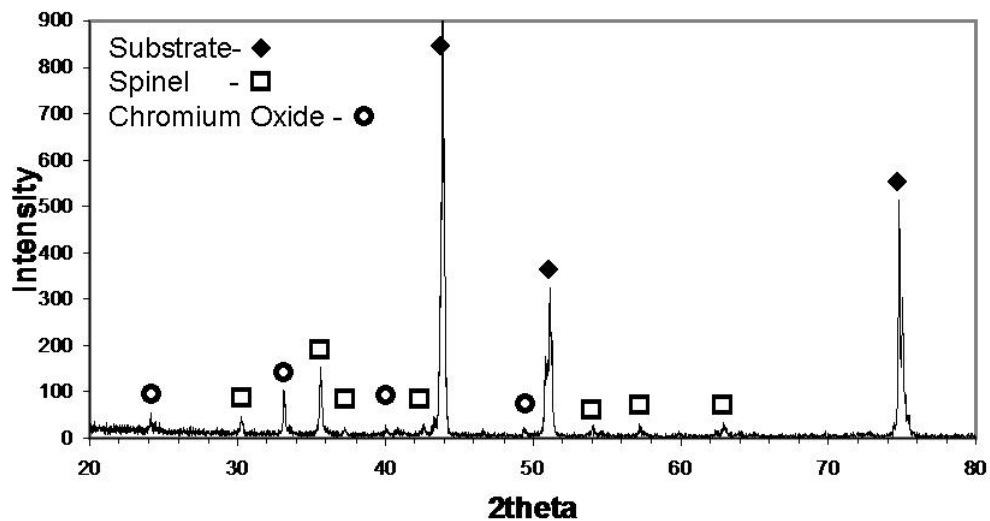

Figure 5. X-Ray Diffraction pattern of an Ni/Fe alloy coated Haynes 230 sample with the alloy having a composition of 25% Ni and 75% Fe after heating in air to 800°C.

Summary

The work presented here has focused on developing a solution composition for electrodeposition of alloys that can then be subsequently oxidized to form protective oxide coatings for low cost metallic interconnects for planar solid oxide fuel cells. It was found that saccharin addition to the deposition solution acts as a leveling agent, leading to much smoother films. It is also necessary to adjust the deposition potentials of the Mn/Co solution by complexation of the Co2+ ion with EDTA and control of the Mn deposition species by adjusting the pH of the solution. In the case of the Ni/Fe solution, the relatively close standard reduction potentials for Ni and Fe means that chelation of the Ni^{2+} cation by EDTA suffices to adjust the deposition potential for the alloy solution. For the Mn/Co alloy deposition it is important to take care not to drive the water splitting reaction so fast that localized pH levels cause hydroxide formation on the work piece. We have begun studying the oxidation process for the deposited

alloys, and thus far spinel phases have been detected by XRD after the alloy coated samples. It is not clear at this time what specific spinel has formed and further analysis by SEM and EDS will be accomplished.

In future work we will continue to address the oxidation of the electrodeposited alloys and we wil evaluate the effectiveness of the oxide coatings as protective layers by measuring area specific resistance and by testing coated samples in contact with SOFC button cells.

References

1. S.C. Singhal, *Solid State Ionics*, 2000, 135, 305-313

2. W.Z. Zhu, S.C. Deevi, *Materials Science and Engineering,* 2003, A348, 227-243

3. K. Fujita, K. Ogasawara, Y. Matsuzaki, T. Sakurai, *J. of Power Sources*, 2004, 131, 261-269

4. S. Taniguchi, M. Kadowaki, H. Kawamura, T. Yasuo, Y. Akiyama, Y. Miyake, T. Saitoh, *J. of Power Sources*, 1995, 55, 73-79

5. S. Linderoth, Controlled reactions between chromia and coatings on alloy surface, *Surface and Coating Technology*, 1996, 80, 185-189

6. J. Kim, R, Song, S. Hyun*, Solid State Ionics*, 2004, in press, available at www.sciencedirect.com

7. X. Chen, P. Hou, C. Jacobson, S. Visco, L. De Jonghe, *Solid State Ionics* 2005, 176, 425-433

8 C. Muller, M.Sarret, and T Andreu, *J. of the Electrochemical Society* (2002), 149 (11) C600-C606